

**SEE THE
POSSIBILITIES**

Amnis® imaging flow cytometers



MILLIPORE
SIGMA

Discover More



The Journal of
Immunology

Computationally Designed Bispecific MD2/CD14 Binding Peptides Show TLR4 Agonist Activity

This information is current as
of December 2, 2018.

Amit Michaeli, Shaul Mezan, Andreas Kühbacher, Doris Finkelmeier, Maayan Elias, Maria Zatsepin, Steven G. Reed, Malcolm S. Duthie, Steffen Rupp, Immanuel Lerner and Anke Burger-Kentischer

J Immunol 2018; 201:3383-3391; Prepublished online 22
October 2018;

doi: 10.4049/jimmunol.1800380

<http://www.jimmunol.org/content/201/11/3383>

**Supplementary
Material** <http://www.jimmunol.org/content/suppl/2018/10/19/jimmunol.1800380.DCSupplemental>

References This article **cites 39 articles**, 9 of which you can access for free at:
<http://www.jimmunol.org/content/201/11/3383.full#ref-list-1>

Why *The JI*? Submit online.

- **Rapid Reviews! 30 days*** from submission to initial decision
- **No Triage!** Every submission reviewed by practicing scientists
- **Fast Publication!** 4 weeks from acceptance to publication

**average*

Subscription Information about subscribing to *The Journal of Immunology* is online at:
<http://jimmunol.org/subscription>

Permissions Submit copyright permission requests at:
<http://www.aai.org/About/Publications/JI/copyright.html>

Email Alerts Receive free email-alerts when new articles cite this article. Sign up at:
<http://jimmunol.org/alerts>

The Journal of Immunology is published twice each month by
The American Association of Immunologists, Inc.,
1451 Rockville Pike, Suite 650, Rockville, MD 20852
Copyright © 2018 by The American Association of
Immunologists, Inc. All rights reserved.
Print ISSN: 0022-1767 Online ISSN: 1550-6606.



Computationally Designed Bispecific MD2/CD14 Binding Peptides Show TLR4 Agonist Activity

Amit Michaeli,* Shaul Mezan,* Andreas Kühbacher,[†] Doris Finkelmeier,[†] Maayan Elias,* Maria Zatsepin,* Steven G. Reed,[‡] Malcolm S. Duthie,[‡] Steffen Rupp,^{†,§} Immanuel Lerner,* and Anke Burger-Kentischer^{†,§}

Toll-like receptor 4 plays an important role in the regulation of the innate and adaptive immune response. The majority of TLR4 activators currently in clinical use are derivatives of its prototypic ligand LPS. The discovery of innovative TLR4 activators has the potential of providing new therapeutic immunomodulators and adjuvants. We used computational design methods to predict and optimize a total of 53 cyclic and linear peptides targeting myeloid differentiation 2 (MD2) and cluster of differentiation 14 (CD14), both coreceptors of human TLR4. Activity of the designed peptides was first assessed using NF- κ B reporter cell lines expressing either TLR4/MD2 or TLR4/CD14 receptors, then binding to CD14 and MD2 confirmed and quantified using MicroScale Thermophoresis. Finally, we incubated select peptides in human whole blood and observed their ability to induce cytokine production, either alone or in synergy with LPS. Our data demonstrate the advantage of computational design for the discovery of new TLR4 peptide activators with little structural resemblance to known ligands and indicate an efficient strategy with which to identify TLR4 targeting peptides that could be used as easy-to-produce alternatives to LPS-derived molecules in a variety of settings. *The Journal of Immunology*, 2018, 201: 3383–3391.

Toll-like receptor 4 plays a fundamental role in pathogen recognition and activation of innate immunity. TLR4 signaling is dependent on the coreceptors MD2 and CD14 that bind LPS and facilitate TLR4 dimerization and MD2/TLR4 and CD14/TLR4 complex formation, followed by downstream signaling (1). The receptor's prototypic ligand is LPS, found in most gram-negative bacteria. Emanating from the classical role of TLR4 in sensing LPS and mediating immunological response against invading bacteria (2), refined TLR4 activators are primary candidates for use as vaccine adjuvants. Indeed, several LPS derivatives are approved for clinical use (3). TLR4 signaling also plays a role in mediating nonbacterial pathologies and a wide array of pathophysiological conditions. Moreover, the potential of

TLR4 activation has been shown for treatment of neuropathic pain (4), insulin resistance (5), ischemia-related injuries of various types (6–8), autoimmune disorders (1), and cancer immunotherapy (9, 10).

Most known LPS-derived TLR4 activators are, however, unfit for use as adjuvants and immunotherapy agents because of their toxicity, poor efficacy, difficulties in their synthesis, and/or prohibitive manufacturing costs. Therefore, numerous efforts are being made to discover novel TLR4-activating molecules. In a recent effort, high throughput screening of a ~90,000 small molecule library enabled the discovery of neoseptins as synthetic agonists of TLR4. These small molecules bear no relation to LPS and bind the murine, but not the human, MD2 coreceptor and activate it in the micromolar range (11). Using an alternate approach, a rational redesign of peptides that interact with the TLR4/MD2 binding interface was performed (12). This yielded macrocyclic peptides that, although they failed to facilitate TLR signaling when administered alone, showed some synergy when coadministered with LPS. Other past discovery efforts included phage display, yielding 6- μ M active natural linear peptide activators of TLR4 (13).

Using a specific *ab initio* computational approach for the design of novel active peptides previously used in the design of a protein stabilizing peptide LTKE based solely on the glycogen-branching enzyme 1 (GBE1) protein structure (14), we designed and modified novel linear and cyclic peptides to interact with the binding pocket of the human TLR4 coreceptors MD2 and CD14. Despite their lack of resemblance to LPS or its derivatives, each peptide was able to activate the TLR4 signaling pathways in a cell-based reporter gene setting (15). We then determined the binding affinity (K_d) for three lead peptides (two cyclic and one linear) using MicroScale Thermophoresis (MST) and further evaluated their activity under physiologically relevant conditions by determining IL-1 β release upon culture in human whole blood. We observed that two of the three peptides induced IL-1 β release when applied alone, and each demonstrated a strong synergistic effect when cocubated with LPS. Together, our results demonstrate the

*Pepticom Ltd., Givat-Ram, 9139002 Jerusalem, Israel; [†]Fraunhofer Institute for Interfacial Engineering and Biotechnology IGB, 70569 Stuttgart, Germany; [‡]Infectious Disease Research Institute, Seattle, WA 98102; and [§]Institute of Interfacial Process Engineering and Plasma Technology, University of Stuttgart, 70569 Stuttgart, Germany

ORCID: 0000-0002-4083-2050 (A.K.).

Received for publication March 12, 2018. Accepted for publication September 20, 2018.

This work was supported by the Eureka Project, Denosyntrac (Project 8 829).

A.M. performed the computational design of peptides, analyzed the data, and wrote the paper. S.M. analyzed the data and wrote and edited the paper. S.R. team conceived, designed, and performed the experiments and analyzed the data. S.G.R. and M.S.D. helped in the editing and revision of the paper. I.L. and S.R. wrote the paper and supervised the work.

Address correspondence and reprint requests to Dr. Immanuel Lerner, Dr. Anke Burger-Kentischer, or Prof. Steffen Rupp, Pepticom Ltd., Hi-Tech Park, Edmond J. Safra Campus, Givat-Ram, 9139002 Jerusalem, Israel (I.L.) or Fraunhofer IGB, Nobelstrasse 12, 70569 Stuttgart, Germany (A.B.-K. and S.R.). E-mail addresses: immanuel.lerner@pepticom.com (I.L.), anke.burger-kentischer@igb.fraunhofer.de (A.B.-K.), or steffen.rupp@igb.fraunhofer.de (S.R.)

The online version of this article contains supplemental material.

Abbreviations used in this article: 3D, three-dimensional; MST, MicroScale Thermophoresis; PAMP, pathogen-associated molecular pattern; PDB, Protein Data Bank; RMSD, root mean square deviation; SEAP, secreted alkaline phosphatase.

Copyright © 2018 by The American Association of Immunologists, Inc. 0022-1767/18/\$37.50

efficiency of using a computational method that employs solved three-dimensional (3D) structures of target receptors for the discovery of unique peptides with binding potential. The TLR4 peptide agonists discovered and described in this study can potentially be developed as novel adjuvants and immunomodulators.

Materials and Methods

Input protein structure and analysis

Peptides were designed using Pepticom's proprietary ab initio design software based on atomic resolution 3D structures of the targeted protein. As an initial input, structures of the human TLR4/MD2 complex bound to either the antagonist eritoran (Protein Data Bank [PDB]: 2Z65) (16) or the natural agonist LPS (PDB: 3FXI) (17) were analyzed. The CD14 input structure selected was of its human unbound structure (PDB: 4GLP) (18). The hydrophobic N terminus pocket was also modeled using the unbound murine structure (PDB: 1WWL) (19). Structure comparisons and visualization were performed using the PyMOL Molecular Graphics System, Version 1.8; Schrödinger (New York, NY). Protein loop and homology modeling were performed using the Prime suit (Schrödinger Release 2017-1: Prime, Schrödinger, 2017) (20, 21).

Design of potential TLR4 coreceptor binding peptides

Linear and cyclic peptides were designed using Pepticom's software. Both LINEPEP and CYCEP protocols use the risk-adjusted design algorithm (22) based on risk-return heuristics of the Modern Portfolio Theory (23). In brief, the risk-adjusted design algorithm calculates a potential "reward" or "return" for every variable value in an equation while assessing the "risk" associated with the selection of that variable value. Values are only stochastically selected if no other values that have better return for a similar risk or lower risk for similar returns exist. For example, returns or rewards can include the binding free energy component calculated for the variable value (i.e., side chain composition in a discrete orientation and point in space). Whereas the risk associated with the variable value can be the sum of all returns, which are incompatible and hence mutually exclusive with that value (i.e., the average binding energy components of all other side chain compositions in all orientation and point in space, which clash with a particular side chain composition). This heuristic has previously been used to design a stabilizing chaperone for the mutant glycogen-branching enzyme 1 (hGBE1) (14).

Peptides

Lyophilized peptides were produced at EMC Microcollections (Tubingen, Germany) and stored at -20°C until use. Peptides were reconstituted/dissolved in DMSO at a concentration of either 10 mM or otherwise to the highest possible concentration as indicated. Sonication was used to dissolve the peptides if necessary. For each experiment, the stock solution was diluted in DMEM to the appropriate working concentration (between 1 mM and 0.1 μM). The peptides are diluted in such a way that the final DMSO concentration in minimal media did not exceed 0.1%.

Cell-based innate immune receptor assay

Designed peptides were tested for activation of TLR4 signaling pathway using a cell-based assay for detection of pathogen-associated molecular pattern (PAMP), as previously described (15, 24). NIH-3T3 cells (mouse fibroblasts) stably transfected with an NF- κB activity transcriptional reporter (based on endothelial cell leukocyte adhesion molecule 1 [ELAM1] proximal promoter that combines five NF- κB binding sites) with secreted alkaline phosphatase (SEAP) was used in combination with TLR4 and its coreceptors: either TLR4/MD2 or TLR4/CD14. Cells were cultured in 20 ml of culture media (DMEM supplemented with 10% FCS [heat inactivated], 50 U/ml penicillin, 0.05 mg/ml streptomycin, and 2 mmol/l L-glutamine) in a standard cell culture flask (75-cm² T-Flask) at 37°C in a 5% CO₂-humidified atmosphere. For assay, cells were transferred into 96-well plates at a density of 3×10^4 cells/well in a final volume of 100 μl culture media (DMEM, 10% FCS [heat inactivated]). After incubating for 24 h, the media was replaced with the respective volume of fresh media (DMEM, 0.5% FCS [heat inactivated]) and peptides, TLR4 agonist, or a mixture of both were added in a serial dilution to provide a final volume of 100 μl /well. Cells incubated in culture medium containing only 0.5% FCS were used as a negative reference. Incubations were performed for 18 h at 37°C and 5% CO₂. To determine receptor engagement and NF- κB induction, 50 μl of culture supernatant was carefully transferred to a new 96-well plate (Greiner F-plate) and 50 μl of the substrate p-nitrophenyl phosphate added. SEAP catalyzes the hydrolysis of p-nitrophenyl phosphate

to the final product paranitrophenol (yellow), which was detected by a photometric analysis using a UV/visible reader at 405 nm 1 h after the reaction was initiated.

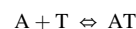
EC₅₀/IC₅₀ calculations

Absolute EC₅₀/IC₅₀ values were estimated by determining the point corresponding to 50% activity in our cell based assay (the mean of the no treatment and LPS controls used; 0 and 100% activity, respectively). Peptide concentration corresponding to 50% activation by LPS was then extrapolated from its dose/response curve. Relative EC₅₀/IC₅₀ concentrations were determined as those corresponding to a response midway between the estimates of the lower and upper plateaus of the peptide dose/response curve. The model used for the drug response analysis was the Richard (25) equation, also referred to as a five-parameter logistic regression. A fitted line was extrapolated using a weighted four-parametric logistic regression, in R, using the nplr package, version 0.1.7. EC₅₀ values were derived from the resulting equation by solving it to the point where the tested peptide caused 50% activation.

Fluorescent MST

Peptide K_d to their target protein were determined using a MST binding assay performed by 2Bind molecular interaction services (Regensburg, Germany). The MST protocol used for this study was generally described in (26, 27). For protein labeling, MD2 and CD14 (R&D Systems, Minneapolis, MN) were labeled using Monolith Protein Labeling Kit RED-NHS (NanoTemper Technologies) according to the manufacturer's instructions in the supplied labeling buffer. After labeling, the protein was eluted into 1× PBS (pH 7.4) including 0.1% Pluronic F-127. MST binding experiments were conducted with 1 nM of NT647-labeled protein in binding buffer (1× PBS [pH 7.4], 0.1% Pluronic F-127, and 5% DMSO) with concentrations ranging from 0.031 to 100,000 nM at 80% MST power, 20% light-emitting diode power in premium coated capillaries on a Monolith NT.115 pico device at 25°C (NanoTemper Technologies, Munich, Germany). Data were analyzed using MO.Affinity Analysis software (version 2.2.4; NanoTemper Technologies) at the standard MST time of 30 s (respectively thermophoresis plus T-jump). The K_d of the interaction was determined by fitting the data using MST standard fit algorithm derived from the law of mass action. To calculate fraction bound, the ΔF_{norm} value of each point was divided by the amplitude of the fitted curve, resulting in values from 0 to 1 (0 = unbound, 1 = bound) and processed using the KaleidaGraph 4.5 software and fitted using the K_d fit formula derived from the law of mass action. Error bars represent the SD of two independent experiments, each with two technical repeats.

Curve fit formula. The K_d from the law of mass action was as follows:



$$\text{Fraction bound} = \frac{1}{2c_A} \left(c_T + c_A + K_d - \sqrt{(c_T + c_A + K_d)^2 - 4c_Tc_A} \right)$$

where K_d is to be determined; c_A indicates the constant concentration of molecule A (fluorescent), known; and c_T indicates the concentration of titrated molecule T.

The fitting model from the law of mass action is considered as correctly describing data when a molecule A interacts with a molecule B using one binding site or using multiple binding sites with the same affinity.

Peptide activity in human blood

For the assessment of selected peptides in blood, peptides were incubated in human blood at EC₅₀ values previously obtained in PAMP assays as well as twice and half this concentration. Ten-milliliter Stock solutions of peptide in DMSO were diluted in RPMI 1640 to 20 times the final desired concentration. LPS stock solution in water was prediluted in RPMI 1640 to a concentration 2 EU/ml then serially diluted 1:2 in RPMI 1640 to obtain additional standard concentrations of 1, 0.5, 0.25, and 0.125 EU/ml. The study was approved by the institutional scientific and ethics committees. Written informed consent was obtained from all subjects, in total three healthy (two females, one male) volunteers (age 25–35 y). Medical histories and yearly mandatory medical examination of Fraunhofer staff were all normal.

Fresh human blood from three volunteers was diluted 1:10 in RPMI 1640, and 200 μl were added to each well of three 96-well tissue culture plates, then 10 μl of one of the compounds or 10 μl RPMI 1640 medium was added. Additionally, 10 μl LPS (1 EU/ml) or mock RPMI 1640 was added; each condition was tested in triplicates. A standard concentration series of LPS was prepared in separate wells by adding 10 μl of LPS at

concentrations of 2 EU/ml to 0.125 EU/ml. Plates were then incubated at 37°C in a humidified 5% CO₂ atmosphere for 24 h. To determine biological responsiveness, 150 μ l of culture supernatant was transferred from each well to a new 96-well plate and stored at -20°C until IL-1 β was measured by ELISA according to the manufacturer's instructions (Human IL-1 β ELISA Kit, ab46052; Abcam; Cambridge, MA). Absorbance was measured at a wavelength of 450 nm. IL-1 β concentrations were calculated by extrapolation against the IL-1 β standard dilution series.

Naphthol blue/black staining

For evaluating the cytotoxic effects of peptides, cells were fixed with 4% paraformaldehyde for 30 min directly after performing the PAMP assay with the cell culture supernatant. Subsequently, cells were stained with 50 μ l of naphthol blue/black solution (0.05% naphthol blue/black, 9% acetic acid, and 0.1 M sodium acetate) per well, washed under running deionized water, and air dried. The dye was then solubilized by adding 100 μ l or 0.1 M NaOH, and the absorption at 650 nm was measured using a plate reader.

Results

MD2 and CD14 structure analyses suggest respective rigid and multiconformational models for peptide design

Ab initio discovery focuses on the target protein structure rather than the structure and properties of known ligands, so for the purpose of ab initio discovery of novel potential TLR4-binding molecules, we examined known structures of TLR4 and its coreceptors. Different solved structures of the MD2 binding pocket were compared. These analyses revealed that MD2 binding pocket backbone conformation remained conserved in human structures bound to the agonist LPS (PDB: 3FXI) (17) and the antagonist eritoran (PDB: 2Z65) (16) and in murine structures, either unbound (PDB: 5IJB) or bound to neoseptin-3 (PDB: 5IJC) (11) with the backbone root mean square deviation (RMSD) remaining below 1.5 Å from one another and without noticeable pocket constrictions. For example, superimposing the human receptor bound with LPS and with the less restrictive myristic acid (PDB: 2E56) (28) returned an overall RMSD of 0.7 Å and indicated the lack of pocket constriction, because the myristic acid bound structure was also compatible with binding of LPS (Fig. 1A, 1C, left panel). The relatively minor deviations allowed us to hypothesize a rigid backbone model and to initiate peptide discovery without further target protein modeling. Unlike the solved structure for LPS/TLR4/MD2 (17), which shows both elaborate hydrophobic interaction with the pocket of MD2 and hydrogen bond pattern with TLR4, the neoseptin/TLR4/MD2 showed much fewer hydrogen bonds with TLR4 (11). This led us to hypothesize that coreceptor/ligand interactions were primarily responsible for TLR4 activation, which is the reason that we based our peptide discovery on the coreceptor pockets without modeling TLR4 itself.

The hydrophobic N-terminal pocket of the human CD14 structure (PDB: 4GLP) (18) was found to be too constricted to permit effective docking of the LPS molecule taken from the solved LPS/MD2 crystal (PDB: 3FXI) (17) (Fig. 1B, top left). This suggested that a conformational change is required for LPS to bind the N-terminal pocket (Fig. 1B, right panel, blue arrow). In comparison, the unbound murine CD14 structure (PDB: 1WWL) (19) (Fig. 1B, bottom left) was found to be significantly less constricted, although it retained an overall RMSD of 1.4 Å. The primary cause for the pocket constriction in the human structure appears to be a loop formed by residues 66–76 (Fig. 1B, top left, red rectangle), whereas the corresponding residues in the murine structure (46–58) form a more tightly packed α -helix conformation (Fig. 1B, bottom left, red rectangle).

To prepare a nonconstricted human model, the human sequence from the solved structure was threaded onto the murine backbone with the two proteins showing a 66% sequence identity, 77%

similarity, and 3% of gaps caused by a shortage of 6 aa in the human model. The human sequence based on the murine structure was able to fit onto a helical conformation of residues 66–76 using the knowledge based model or alternately to a nonconstrictive loop conformation using the energy based model (20, 21) (Fig. 1B, bottom right panel; Fig. 1C, bottom right panel). The noted deviations between the murine and human unbound CD14 structures, coupled by their sequence compatibility, led us to hypothesize a flexible backbone model and design being performed on multiple backbone conformations in parallel. Overall, our analyses based on the atomic resolution 3D structures of MD2 and CD14 suggested that assuming respective rigid and flexible backbone models was required for the ab initio design of peptide ligands.

Cyclic peptides designed to bind TLR4/MD2 and TLR4/CD14

Head to tail (N–C) cyclization provides protection from exopeptidases and more target specificity because of the more restricted backbone conformation. The additional inclusion of nonnatural amino acids and D-amino acids to the cyclic peptide should maximize its “drug likeness” (29). An innovative cyclic peptide screening library was therefore generated using the CYCPEP discovery module based on the input structures described in Fig. 1. To increase the possibility of discovering peptides that will target both MD2 and CD14, the CYCPEP discovery module was applied on an MD2-centered grid and then on CD14-centered grids. In addition, a solution space restricted to N–C cyclic peptides of a backbone length ranging from 5 to 14 aa was defined. The solution space was restricted to either L- or D-amino acids, in separate runs. The final output consisted of 26 peptides (Table I).

To determine whether a certain designed peptide activated or inhibited TLR4 signaling in a reporter cell assay, we evaluated the proportion between peptides' activity at high (~0.1–0.2 mM) and low (~0.1–0.2 μ M) concentrations. To identify antagonist, we added LPS and the compound, or LPS alone as a control, for identification of agonist only the compound to be tested was added. According to this rational, a high dose/low dose proportion >1 or <1 would suggest an agonist or an antagonist activity, respectively (Fig. 2A, bars coming up and down, respectively). To limit the number of compounds to follow up a cutoff of 2-fold change was set to determine agonist and antagonist activities, 14 of the 26 cyclic peptides showed activity on either TLR4/MD2 or TLR4/CD14 cell lines and could be assigned as activators or inhibitors. For example, PTC–A-40, PTC–A-41, and PTC–A-42 activated if added in the presence of CD14, and even with LPS present, suggesting these are strong CD14 agonists. Conversely, the contradictory actions of PTC–A-50 on the two coreceptors did not allow us to accurately determine its activity. In sum, 11 of the 26 peptides exhibited activity on both TLR4/MD2 and TLR4/CD14 cell lines (Table I, bold).

We then determined the dose/response curve for each peptide to more fully assess their bioactivity. We extrapolated the absolute EC₅₀/IC₅₀ values for the 11 peptides by contrasting against negative and positive controls (Table I, bold). Five out of the 11 peptides exhibited bioactivity below a preset cutoff of EC₅₀/IC₅₀ \leq 50 μ M on both TLR4/MD2 and TLR4/CD14 reporter cell lines (Fig. 3; Supplemental Fig. 1; Table I). Of these, four peptides were considered as agonists: c[MLSF β RM] (PTC–A-40), c[LRGTFIGMWGWMQK] (PTC–A-62), c[gwlwrs] (PTC–A-77), and c[gfwseeeksl] (PTC–A-83), and one was considered to be an antagonist: c[gwwwral] (PTC–A-78). PTC–A-62 reached EC₅₀ values of 10 and 4 μ M in the MD2 and CD14 cell lines, respectively, but was shown to be toxic at 100 μ M (Supplemental Fig. 1A). This toxicity explains the inhibitory effect we observed for PTC–A-62 when calculating its high dose/low dose activity proportion (Fig. 2A). The cyclic D-amino acid, PTC–A-77 activated the MD2

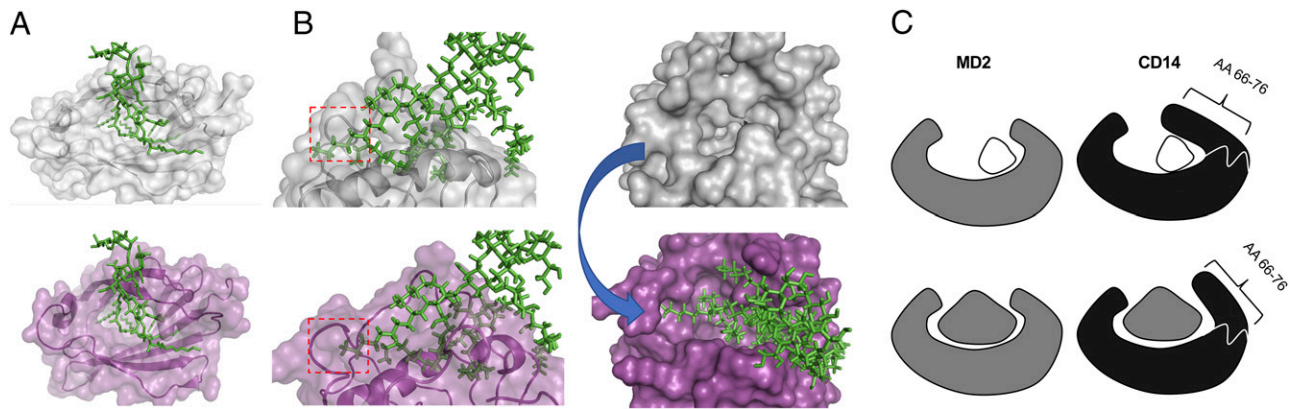


FIGURE 1. MD2 and CD14 structure analyses suggest respective rigid and multiconformational models for peptide design (A). The human MD2 coreceptor was cocrystallized with LPS (PDB: 3FXI) (top; white) and with the less restrictive myristic acid (PDB: 2E56) (bottom; purple). The structures show an overall RMSD of 0.7 Å. The myristic acid bound structure is also compatible with binding LPS (green). (B) Docking of solved LPS (green) taken from the LPS/MD2 crystal (PDB: 3FXI) with the hydrophobic human CD14 binding pocket (PDB: 4GLP) (top left; white) and with the murine CD14 pocket (PDB 1WWL) (bottom left; purple). The structures show an overall RMSD of 1.4 Å. Difference in the conformation adopted by human residues 66–76 that form a constrictive loop (top left; red rectangle) and by the corresponding residues 46–58 in the LPS, accommodating murine helix (Bottom left; red rectangle). A conformational change (right panel; blue arrow) is required for human CD14 (top right) in order for LPS to bind to its hydrophobic N-terminal pocket, as modeled by threading the human sequence to the murine backbone of CD14 (bottom right), which is compatible with LPS binding (green), as demonstrated via docking. (C) A simplified schematic model of MD2 and CD14 coreceptors, illustrating conformational change upon ligand binding. MD2 (left panel) is modeled to bind both large and small ligands (shown as large gray and small white shapes, respectively) in the same conformation, whereas CD14 (right panel) was modeled to modify its conformation to accommodate larger ligands via residues 66–76 (bottom right panel).

and CD14 cell lines with EC_{50} values of ~ 30 and $10 \mu\text{M}$, respectively, but also had a reduced activity at $100 \mu\text{M}$ (Supplemental Fig. 1B). The cyclic D-amino acid PTC-A-78, of similar composition, rather inhibited the MD2 reporter cell line with an approximate EC_{50} value

of $50 \mu\text{M}$ and that of CD14 with an approximate EC_{50} value of $20 \mu\text{M}$ (Supplemental Fig. 1C). The most promising agonist cyclic peptides that were selected for further evaluation were PTC-A-40 and PTC-A-83. PTC-A-40 had MD2 and CD14 EC_{50} values of ~ 4.0 and

Table I. Designed N-C cyclic peptides and corresponding cell culture activities and absolute EC_{50} estimates

No.	Name	Sequence	Activity		EC_{50}/IC_{50} (μM)	
			CD14	MD2	CD14	MD2
1	PTC-A-40^a	c[MLSFRM]^a	A	A	2	4
2	PTC-A-41	c[WMLGMESI]	A	n.a.		
3	PTC-A-42	c[IGFMMMKKEF]	A	A	10	ND
4	PTC-A-43	c[WGMAEMD]	n.a.	n.a.		
5	PTC-A-44	c[SWEFLW]	I	I	200	30
6	PTC-A-45	c[LIWSEGGKW]	n.a.	n.a.		
7	PTC-A-46	c[SIWDTMW]	n.a.	I		
8	PTC-A-50	c[FGGILLR]	ND	ND		
9	PTC-A-51	c[MMMGTR]	A	A	200	ND
10	PTC-A-52	c[FWMSKF]	n.a.	n.a.		
11	PTC-A-53	c[FWVEYGGW]	n.a.	n.a.		
12	PTC-A-54	c[MGLTF]	n.a.	n.a.		
13	PTC-A-55	c[MPMMK]	n.a.	n.a.		
14	PTC-A-56	c[WPPTR]	n.a.	n.a.		
15	PTC-A-57	c[MIMWEGEG]	n.t.	n.t.		
16	PTC-A-58	c[SWSWW]	n.a.	n.a.		
17	PTC-A-60	c[IWSRSW]	n.a.	n.a.		
18	PTC-A-62^a	c[LRGTFIGMWGMQK]^a	A	A	4	10
19	PTC-A-76	c[gwgewth]	A	A	70	ND
20	PTC-A-77^a	c[gwlwrs]^a	A	A	10	30
21	PTC-A-78^a	c[gwwwral]^a	I	I	20	50
22	PTC-A-80	c[geldkftm]	A	A	50	100
23	PTC-A-81	c[gfwsewekw]	n.a.	n.a.		
24	PTC-A-82	c[gwypr]	A	n.a.		
25	PTC-A-83^a	c[gfwseeeksl]^a	A	A	8	4
26	PTC-A-84	c[AFRMTMFI]	A	A	85	100

Activity was determined using the TLR4/NIH-3T3 reporter gene cell lines expressing either the CD14 or MD2 coreceptors with an NF- κ B transcriptional reporter expressing SEAP as described in Fig. 2. The 11 peptides that caused at least 2-fold change in reporter activity in both TLR4/MD2 and TLR4/CD14 reporter cell lines are marked in bold and are considered to be an activator (A) or inhibitor (I). Their absolute EC_{50}/IC_{50} values were estimated by determining the point corresponding to 50% activity in our cell based assay (the mean of the no treatment [0% activity] and LPS [100% activity] controls used). Peptide concentration corresponding to 50% activation by LPS was then extrapolated from its dose/response curve. Lowercase letters represent D-amino acids.

^aThe five peptides having an EC_{50}/IC_{50} value $\leq 50 \mu\text{M}$ for both TLR4/MD2 or TLR4/CD14 reporter cell lines. Their dose/response curves are presented in Fig. 3A and 3B and in Supplemental Fig. 1.

A, activator; c, cyclic; I, inhibitor; n.a., no activity; n.t., not tested.

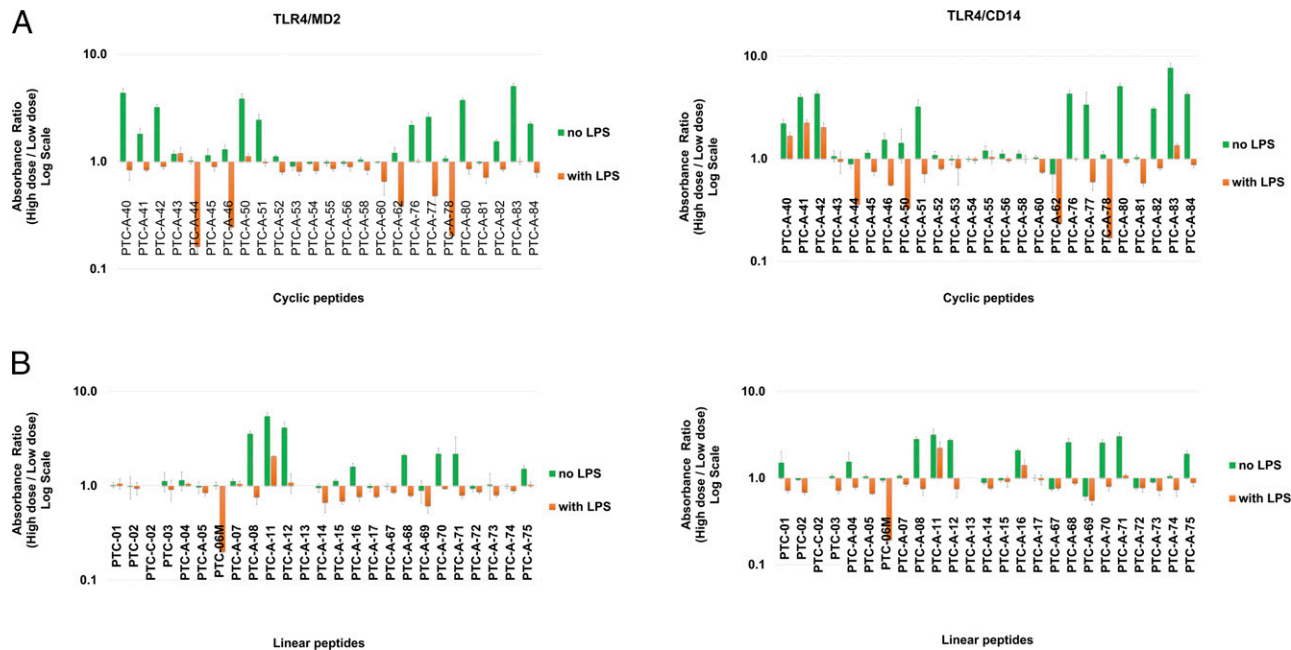


FIGURE 2. Screening of cyclic and linear peptides for their activities. NIH-3T3 cells stably carrying an NF- κ B activity transcriptional reporter with SEAP were used in combination with TLR4 and its coreceptors: either TLR4/MD2 (left) or TLR4/CD14 (right). The activity of both cyclic (**A**) and linear (**B**) peptides was screened. Each cyclic peptide was incubated with cells at two doses: a high concentration corresponding to 0.1 mM (PTC-A-40:PTC-A-51) and 0.2 mM (PTC-A-52:PTC-A-84) and at a second 1:1000 dilution low concentration corresponding to 0.1 (PTC-A-40:PTC-A-51) and 0.2 μ M (PTC-A-52:PTC-A-84). These were given both alone (green bars) or mixed with a saturating dose of 25 ng/ml LPS (red bars), except for the cyclic peptides PTC-A-52:PTC-A-84 that, when tested on MD2, were mixed only with 10 ng/ml LPS. Linear peptides were also applied at high and low concentrations corresponding to 0.1 mM and 0.1 μ M, respectively, except for PTC-A-14:PTC-A-17 that were applied at 0.15 mM and 1.5 μ M (1:100 dilution). LPS was mixed with all linear peptides at concentration of 50 ng/ml except when mixed with (PTC-A-67:PTC-A-71) at 25 ng/ml. For each peptide, the ratio between activity at high and low concentration was calculated and is presented on a logarithmic scale. A cutoff of 2-fold change in the proportion between activity at high and low concentration was used to determine agonist and antagonist activities for the 26 cyclic (see Tables I and II for the determined activities of the 26 cyclic and 26 linear peptides, respectively). Three independent experiments were performed. Results presented are of one representative experiment. Error bars represent SD of three technical repeats.

2.0 μ M (Fig. 3A), whereas PTC-A-83 had MD2 and CD14 EC_{50} values of \sim 4.0 and 8.0 μ M (Fig. 3B). To exclude potential cytotoxic effects of the PTC-A-40 and PTC-A-83, cells were stained with naphthol blue/black after treatment with the ligands and performance of the PAMP assay. As shown in (Supplemental Fig. 4A, 4B), all three peptides PTC-A-40, PTC-A-83, and PTC-A-12M1 did not result in cell death at any tested concentration.

To provide evidence that the activity of the PTC-A-40 and PTC-A-83 peptides was due to specific and direct binding to TLR4 coreceptors and to determine K_d of such binding, we performed fluorescent MST in the presence of MD2 or CD14 (Fig. 4A, 4B, respectively). Interestingly, the calculated K_d values indicate that the designed peptides have high binding affinities for CD14 (Table II). The cyclic L-amino acid PTC-A-40 had a K_d of 3.5 ± 0.9 μ M to MD2 and 163 ± 67 nM to CD14. The cyclic D-amino acid PTC-A-83 had a K_d of 8.0 ± 2.3 μ M to MD2 and 189 ± 70 nM to CD14. By comparison, the K_d for the bacterial LPS was also determined, showing a K_d of 13.0 ± 3 nM to MD2 and 5.0 ± 2 nM to CD14. These results suggest that the CD14 receptor is more “promiscuous” for peptide binding than MD2, possibly because of its previously noted pocket flexibility.

We hypothesized that the methionine residues of the cyclic PTC-A-40 c[MLSFRM] bind the hydrophobic pockets of MD2/CD14 similarly to the hydrophobic lipid chains previously shown by cocrystallization with LPS (30) and eritoran (16). L-Norleucine is a more hydrophobic structural analog of methionine in which the sulfur atom is replaced with a CH_2 moiety and, hence, more similar to the lipid chains of LPS. A modified c[(L-norleucine)LSFR (L-norleucine)] cyclic peptide analog (PTC-A-40M1) showed more

potent binding to MD2, with a K_d of 289 ± 101 nM, and a somewhat reduced binding to CD14, with a K_d of 262 ± 53 nM, than nonmodified PTC-A-40 (Table II), only partially confirming our hypothesis.

Linear peptides designed to bind TLR4/MD2 and TLR4/CD14

Head to tail cyclic peptides are more conformationally constrained than linear peptides. To, therefore, quantify the impact of these constraints, we also designed and evaluated linear peptides. Linear peptides are freer to reach a backbone conformation that will ideally position the side chains and, hence, can reach better binding affinity components, with the exception of conformational entropy loss. A linear peptide screening library was generated using the LINEPEP discovery module on the input structures described in Fig. 1. The LINEPEP model solution space restricted to linear peptides, of a backbone length ranging from 5 to 14 aa. The solution space was restricted to either L- or D-amino acids in separate runs.

The final output consisted of 17 L-amino acid peptides and nine D-amino acid peptides that were synthesized and screened for activity using the same criteria as was used for the cyclic peptides. Seven of the 26 linear peptides showed activity in both TLR4/MD2 and TLR4/CD14 reporter lines and, with the exception of one peptide (PTC-A-06M), exhibited agonist activities (Fig. 2B; Table III, bold). After extrapolating the absolute EC_{50}/IC_{50} from the dose/response curves for all seven peptides, we focus on peptides PTC-A-08, PTC-A-11, and PTC-A-12, which had EC_{50}/IC_{50} value ≤ 50 μ M for both MD2 and CD14 (Supplemental Fig. 2; Table III). Interestingly, when incubated in the presence of LPS, PTC-A-11

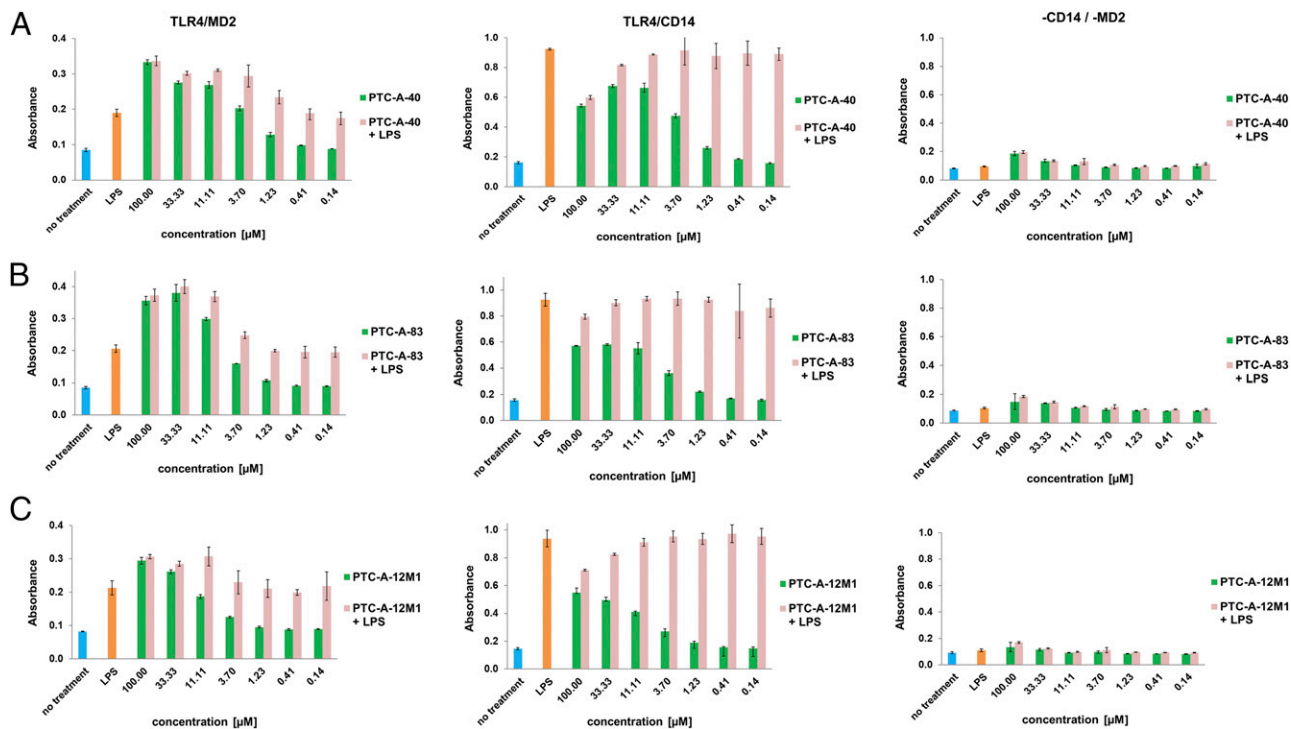


FIGURE 3. Characterization of the agonist activity of selected cyclic and linear peptides on their TLR4 coreceptors. PAMP cell-based assay was used to determine the dose/response curves and estimate EC_{50} values for the cyclic PTC-A-40 (**A**) and PTC-A-83 (**B**) and the linear PTC-A-12M1 (**C**) peptides. The assay was performed on NIH-3T3 cells expressing either TLR4/ MD2 (left panel), TLR4/CD14 (middle) coreceptors, or on control NIH-3T3 cells that do not express either coreceptor (right panel) and reflect background levels of SEAP expression and unspecific activation of the NF- κ B reporter. Peptides were applied at concentration ranging from 0.14 μ M to 0.1 Mm, either alone (green) or mixed with 10 ng/ml LPS (purple), which was also applied by itself as a positive control for 100% activation. No treatment control was used to determine basal levels of reporter activation. Absolute EC_{50}/IC_{50} values were estimated as described in *Materials and Methods* and are listed in Tables I and II. For the relative EC_{50} values extrapolated from the data, see Supplemental Fig. 3. Three independent experiments were performed. Results presented are of one representative experiment. Error bars represent the SD of three technical repeats.

exhibited synergy on both TLR4/MD2 and TLR4/CD14 reporter cells (Supplemental Fig. 2B).

Of the 17 L-amino acid peptides, eight were of a single backbone conformation (pairwise RMSD < 1 Å), 9-aa superfamily, hereby referred to as “Superfamily A.” The Superfamily A backbone had the following composition:

(I/L)₁(L/M)₂(Y/F)₃(M/K)₄(G/S)₅(M/L/N)₆(K/E)₇(W)₈(L/M)₉, with a modeled buried N terminus and solvent-exposed C terminus. PTC-A-11 (ILYMSLKWM) and PTC-A-12 (ILYKSLKWM) belong to Superfamily A. The N terminus of Superfamily A is modeled to be buried in a hydrophobic pocket, without compensating hydrogen bonds, for both MD2 and CD14. This was

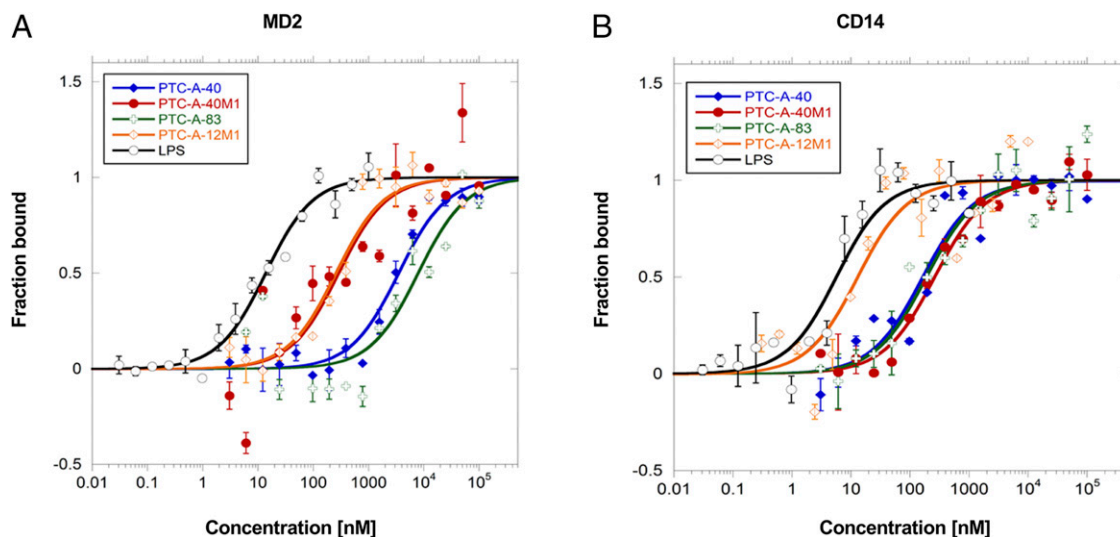


FIGURE 4. MST binding assay. Affinity of the cyclic PTC-A-40 (blue), PTC-A-40M1 (red), and PTC-A-83 (green) and the linear PTC-A-12-M1 (orange) peptides to their target TLR4 coreceptors MD2 (**A**) and CD14 (**B**) was measured and compared with LPS binding (black). Binding affinity is plotted as a fraction bound with values from 0 to 1 (0 = unbound, 1 = bound) against a range of peptide concentrations from 0.031 to 100,000 nM. The K_d of the interaction was determined by fitting the data as described in *Materials and Methods*. K_d values are presented in Table II. Error bars represent the SD of two independent experiments, each with two technical repeats.

Table II. K_d values for the binding of designed peptides to MD2 and CD14 determined by MST

	K_d (nM)
MD2	
LPS	13 ± 3
PTC-A-40	3508 ± 869
PTC-A-40M1	289 ± 101
PTC-A-83	7933 ± 2320
PTC-A-12M1	257 ± 82
CD14	
LPS	5 ± 2
PTC-A-40	163 ± 67
PTC-A-40M1	262 ± 53
PTC-A-83	189 ± 70
PTC-A-12M1	13 ± 9

predicted to contribute a poor desolvation binding energy component when binding both MD2 and CD14. We hypothesized that circumventing this interaction by replacing the N terminus isoleucine with 3-methylpentanoic acid would eliminate the poor desolvation but retain the favorable hydrophobic effect of the isoleucine side chain. We therefore synthesized a 3-methylpentanoic acid modified PTC-A-12 (PTC-A-12M1), then determined its dose/response curve (Fig. 3C) and extrapolated its EC_{50} . Absolute EC_{50} values of PTC-A-12M1 were determined as 5 and 33 μ M for the CD14 and MD2 reporter lines, respectively (Table III, peptide no. 27). These EC_{50} values reflect a significant

improvement over those observed for the unmodified PTC-A-12 (Supplemental Fig. 2C). The relative EC_{50} (Supplemental Fig. 3C) and binding affinity to TLR4 coreceptors (Fig. 4) of PTC-A-12M1 were also determined. The K_d for the binding of the modified peptide to CD14 and MD2 were calculated to be 13 ± 9 nM and 257 ± 82 nM, respectively (Table II).

To exclude the potential cytotoxic effects of PTC-A-12M1, cells were stained with naphthol blue/black after the treatment with the ligands and the performance of the PAMP assay. As shown in (Supplemental Fig. 4C), PTC-A-12M1 did not result in cell death at any tested concentration.

Taken together, these data indicate that both cell activation and binding affinity were significantly higher when PTC-A-12M1 was bound to CD14 rather than MD2.

Indication of responses in primary cells

A well-defined biological effect of LPS binding to TLR4 is the secretion of the proinflammatory cytokines including IL-1 β (31). Quantification of IL-1 β by the monocyte activation test is therefore a robust verified method for the assessment of pyrogens. To evaluate the functional impact of selected peptides in the physiological setting of human blood, they were incubated in whole blood, and the release of IL-1 β was quantified by ELISA. The linear peptide PTC-A-12M1 as well as the two cyclic peptides PTC-A-40 and PTC-A-83 were tested alone and in combination with LPS. Although PTC-A-12M1 was not effective under either condition tested, PTC-A-40 and PTC-A-83 alone showed a dose-dependent

Table III. Designed linear peptides and corresponding cell culture activities and absolute EC_{50} estimates

No.	Name	Sequence	Activity		EC_{50}/IC_{50} μ M	
			CD14	MD2	CD14	MD2
1	PTC-01	YYLLTYG	n.a.	n.a.		
2	PTC-02	ILFMGMKWL ^a	n.a.	n.a.		
3	PTC-C-02	LAWYFGRKIKE	n.t.	n.t.		
4	PTC-03	FMSFAGF	n.a.	n.a.		
5	PTC-A-04	MIHIMMMRG	n.a.	n.a.		
6	PTC-A-05	MIHIMMMR	n.a.	n.a.		
7	PTC-C-06M	KKLMLII (C-terminal CH3 replace COOH)	I	I	100	40
8	PTC-A-07	RYYTYLMMWKG	n.a.	n.a.		
9	PTC-A-08^b	EWGWRMII^b	A	A	50	50
10	PTC-A-11^b	ILYMSLKWM^{a,b}	A	A	50	50
11	PTC-A-12^b	ILYKSLKWM^{a,b}	A	A	50	50
12	PTC-A-13	ILYKSNKWM ^a	n.t.	n.t.		
13	PTC-A-14	ILFKGMKWL ^a	n.a.	n.a.		
14	PTC-A-15	ILFMSMKWL ^a	n.a.	n.a.		
15	PTC-A-16	IMYMSLKWM ^a	n.a.	n.a.		
16	PTC-A-17	LMYKSLEWM ^a	n.a.	n.a.		
17		RMMWFGIMV	n.a.	n.a.		
18	PTC-A-67	kgmlgfik	n.a.	n.a.		
19	PTC-A-68	rmmmw	A	A	30	100
20	PTC-A-69	wwihk	n.a.	n.a.		
21	PTC-A-70	wwikd	A	A	45	100
22	PTC-A-71	etjymmkg	A	A	75	ND
23	PTC-A-72	ppmgmkgea	n.a.	n.a.		
24	PTC-A-73	ywggmkkm	n.a.	n.a.		
25	PTC-A-74	fmmgkh	n.a.	n.a.		
26	PTC-A-75	tiymmtmkg	n.a.	n.a.		
27	PTC-A-12M1 ^b	3-Methylpentanoic acid LYKSLKWM ^b	A	A	5	33

Activity was determined using the TLR4/NIH-3T3 reporter gene cell lines expressing either the CD14 or MD2 coreceptors with an NF- κ B transcriptional reporter expressing SEAP as described in Fig. 2. The 11 peptides that caused at least 2-fold change in reporter activity in both TLR4/MD2 and TLR4/CD14 reporter cell lines are marked in bold and are considered to be an activator (A) or inhibitor (I). Their absolute EC_{50}/IC_{50} values were estimated by determining the point corresponding to 50% activity in our cell based assay (the mean of the no treatment [0% activity] and 10 mg/ml LPS [100% activity] controls used). Peptide concentration corresponding to 50% activation by LPS was then extrapolated from its dose/response curve. Lowercase letters represent D-amino acids.

^aSimilar backbone to Superfamily A.

^bThe four peptides having an EC_{50}/IC_{50} value ≤ 50 μ M for both TLR4/MD2 or TLR4/CD14 reporter cell lines. Their dose/response curves are presented in Supplemental Fig. 2.

A, activator; c, cyclic; I, inhibitor; n.a., no activity; n.t., not tested.

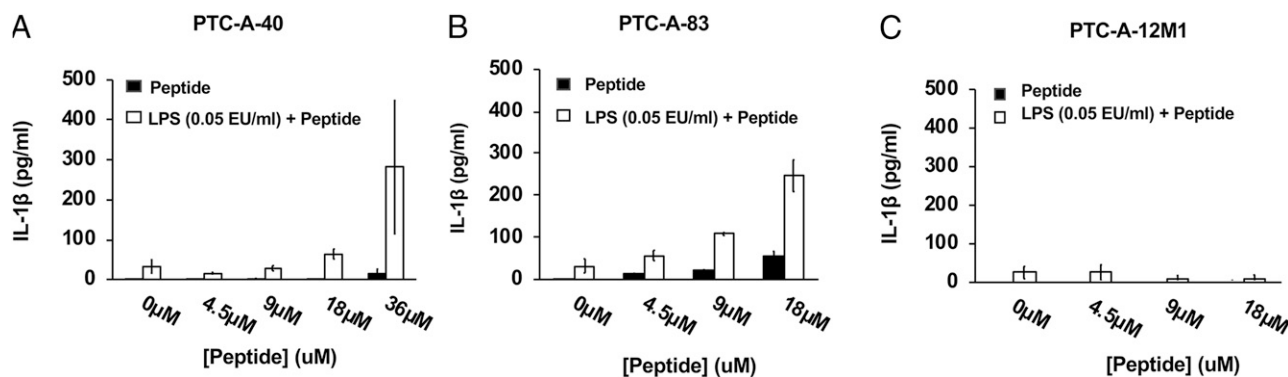


FIGURE 5. Induction of IL-1 β secretion by blood leukocytes upon treatment with synthetic peptides. Secretion of IL-1 β was measured by ELISA in human blood after treatment for 24 h with the peptides PTC-A-40 (A), PTC-A-83 (B), or PTC-A-12M1 (C) at the indicated concentrations alone (black bars) or in combination with 0.05 EU/ml LPS (white bars). Bars represent the mean and SD of results obtained with blood from three voluntary donors each tested in technical triplicates.

elevation of IL-1 β secretion, although for PTC-A-40, a significant increase could only be detected at a concentration of 36 μ M (Fig. 5). Remarkably, in combination with LPS, both cyclic peptides showed a strong synergistic increase of IL-1 β levels. Although the highest IL-1 β concentrations tested with PTC-A-40 and PTC-A-83 alone were 15 and 54 pg/ml, respectively, and LPS treatment resulted in IL-1 β levels between 25 and 32 pg/ml, the latter values increased by 10-fold when blood was treated with a combination of LPS and 36 μ M PTC-A-40 or 18 μ M PTC-A-83 (Fig. 5A, 5B). The peptide vehicle DMSO did not induce IL-1 β secretion at the concentrations used in peptide dilutions as shown in Supplemental Fig. 4D, confirming that the effect was indeed due to the peptides.

Discussion

Identification and synthetic production of TLR targeting molecules has the potential to revolutionize vaccine adjuvants and immune therapeutics. To our knowledge, for the first time, in this study, we demonstrate the efficient prediction and validation of peptides capable of binding to the human TLR4 coreceptor complex. We used a computational *ab initio* strategy to predict a novel, chemically diverse set of peptides with emphasis on the discovery of diverse molecules, differing in length composition and chirality. A total of 26 cyclic and 27 linear peptides were predicted to bind both the CD14 and MD2 coreceptors for TLR4 engagement. Binding of either MD2 or CD14 was first demonstrated for a subset of the peptides by reporter cell assay, then confirmed and further characterized by thermophoresis. Biological evidence of TLR4 agonist activity was demonstrated by culture of peptides PTC-A-83 and PTC-A-40 by incubation with human blood.

Our strategy identified a much higher percentage of active molecules than is observed in high-throughput screening and previous rational design attempts, presumably because of the usage of machine-learning discovery software (22). We believe that the identification of diverse active molecules greatly increases the chance of successfully developing a molecule that can advance to clinical use.

A previous high-throughput screen of small molecules yielded one activator out of 90,000 total peptidomimetic molecules screened, following which structure/activity relationships were used to expand the set to three active neoseptins (11). Binding studies indicated that these molecules bound only the MD2 coreceptor as dimers and did not show CD14 activation (11). Additionally, neoseptins showed no agonist/antagonist activity in human cells unless mouse MD2 was coexpressed. Neoseptins share a peptidomimetic structure composed primarily of nonnatural, aromatic amino acids linked by

amide bonds. This study speculated that short natural peptides could potentially activate the TLR4 receptor via binding of MD2 ligand pocket (11); this is supported by phage display efforts targeted on anti-LPS Abs yielding LPS-mimicking peptides (13). Other discovery efforts have attempted rational design of TLR4 activating peptides using an MD2 coreceptor mimicry approach (12) based on the MD2/TLR4 interface of the solved crystal structure (17). In the case of MD2 mimetics, only disulfide bridge macrocyclic peptides showed agonist activity and only in synergy with LPS, being unable to activate through TLR4 when introduced alone. In contrast, our data show that novel, computationally designed peptides can directly bind and activate TLR4 via both CD14 and MD2 coreceptors.

No sequences in our final output of cyclic and linear peptides were identical, indicating that the cyclic peptides are not derived by cyclization of the linear peptides and demonstrating the independence of the design efforts. Of note, on both CD14/TLR4 and MD2/TLR4 reporter cell lines, the active linear peptides were of much lower potency than the cyclic peptides. The binding model of the dominant linear backbone model, labeled Superfamily A, contained a buried N terminus, without coreceptor polar contact compensation, leading us to hypothesize that removal of the N terminus would improve binding affinity. The replacement of the N terminus isoleucine with 3-methylpentanoic acid led to a significant improvement in reporter gene activation. N-C cyclization eliminates the charges of both termini, and in the case of CD14 and MD2, the burying of these charges in the hydrophobic pocket is likely to be unfavorable for binding. This can theoretically explain the higher potency of the cyclic agonists compared with the unmodified linear peptides. When the charge burial was resolved, the linear peptide benefits from the theoretical advantage of backbone flexibility, allowing them to better fit the coreceptor pockets.

Our findings have several biological implications for potential usage of the peptides identified. TLR4 activation is important in a wide array of pathophysiological conditions, some with no external pathogen involvement (i.e., sterile inflammation) (1, 2, 4–8). TLR4 involvement in diverse pathophysiological conditions ranging from bacterial infections to sterile inflammatory conditions can be explained to a large extent by the danger-associated molecular pattern theory (32–34). Several self-danger-associated molecular pattern activators of TLR4 have been proposed. Among these, HMGB, heat shock proteins, hyaluronan, heparin sulfate, and fibronectin (35) are considerably less potent activators of TLR4 than LPS. In this study, we examined numerous unmodified linear peptides that can activate TLR4 at the micromolar range, primarily centered around Superfamily A and theoretically compatible with natural protein fragments. TLR4 was previously

speculated to be able to bind peptides via the MD2 binding pocket (11, 36). Our results suggesting a wide array of novel TLR4-activating natural peptides (as well as nonnatural active peptides) lend some support to prior speculation that a wide variety of yet undiscovered natural cryptic peptide ligands may exist in the human proteome (36). Such peptides may become available for TLR4 binding and activation in the context of proteolytic degradation under sterile inflammatory conditions (37). Further research is required to reveal if the peptides we identified, or mimetics of them, occur in the human proteome and participate in TLR4 activation under inflammatory conditions.

Interestingly, as indicated by elevated levels in IL-1 β release from human blood cells, a synergistic activity was observed for peptides PTC-A-83 and PTC-A-40 when they were cocubated with LPS. It has been reported that CD14 can act as a coreceptor for both TLR4 and TLR2 depending on the binding molecule/activator, and TLR2 activation by molecules, such as CMV envelope proteins, is greatly enhanced in the presence of CD14 (38, 39). It is therefore possible that, beyond the agonistic binding of TLR4 shown in this study, that peptides PTC-A-83 and PTC-A-40 are also capable of activating cells via the engagement of TLR2 with CD14. This appears to merit further investigation.

In summary, our computational approach proved to be a highly efficient strategy with which to identify potential TLR4 agonists. The ease of synthesis and reduced cost of production relative to LPS-derived molecules indicates the TLR4-activating peptides discovered could potentially be further optimized and used as novel adjuvants/immunomodulators following extensive *in vivo* development for a wide variety of indications.

Acknowledgments

We thank Thomas Schubert from 2Bind GmbH molecular interactions for the MST service. We also thank EMC Microcollections for synthesizing peptides.

Disclosures

I.L. and A.M. are founders and directors of Pepticom Ltd. A.M., I.L., M.Z., S.M., and M.E. are full-time employees of Pepticom Ltd. with stock or options. The results of this research are patent pending, PCT no. WO2017141248, titled "Peptide Agonists and Antagonists of TLR4 Activation." S.R., I.L., A.B.-K., and A.M. are inventors of the patent.

References

- Kawai, T., and S. Akira. 2010. The role of pattern-recognition receptors in innate immunity: update on Toll-like receptors. *Nat. Immunol.* 11: 373–384.
- Poltorak, A., X. He, I. Smirnova, M. Y. Liu, C. Van Huffel, X. Du, D. Birdwell, E. Alejos, M. Silva, C. Galanos, et al. 1998. Defective LPS signaling in C3H/HeJ and C57BL/10ScCr mice: mutations in Tlr4 gene. *Science* 282: 2085–2088.
- Reed, S. G., F. C. Hsu, D. Carter, and M. T. Orr. 2016. The science of vaccine adjuvants: advances in TLR4 ligand adjuvants. *Curr. Opin. Immunol.* 41: 85–90.
- Hutchinson, M. R., Y. Zhang, K. Brown, B. D. Coats, M. Shridhar, P. W. Sholar, S. J. Patel, N. Y. Crysedale, J. A. Harrison, S. F. Maier, et al. 2008. Non-stereoselective reversal of neuropathic pain by naloxone and naltrexone: involvement of toll-like receptor 4 (TLR4). *Eur. J. Neurosci.* 28: 20–29.
- Shi, H., M. V. Kokoeva, K. Inouye, I. Tzamelis, H. Yin, and J. S. Flier. 2006. TLR4 links innate immunity and fatty acid-induced insulin resistance. *J. Clin. Invest.* 116: 3015–3025.
- Tsung, A., R. A. Hoffman, K. Izuishi, N. D. Critchlow, A. Nakao, M. H. Chan, M. T. Lotze, D. A. Geller, and T. R. Billiar. 2005. Hepatic ischemia/reperfusion injury involves functional TLR4 signaling in nonparenchymal cells. *J. Immunol.* 175: 7661–7668.
- Wu, H., G. Chen, K. R. Wyburn, J. Yin, P. Bertolino, J. M. Eris, S. I. Alexander, A. F. Sharland, and S. J. Chadban. 2007. TLR4 activation mediates kidney ischemia/reperfusion injury. *J. Clin. Invest.* 117: 2847–2859.
- Dvoriantschikova, G., D. J. Barakat, E. Hernandez, V. I. Shestopalov, and D. Ivanov. 2010. Toll-like receptor 4 contributes to retinal ischemia/reperfusion injury. *Mol. Vis.* 16: 1907–1912.
- Palucka, K., and J. Banchereau. 2012. Cancer immunotherapy via dendritic cells. *Nat. Rev. Cancer* 12: 265–277.

- Adams, S. 2009. Toll-like receptor agonists in cancer therapy. *Immunotherapy* 1: 949–964.
- Wang, Y., L. Su, M. D. Morin, B. T. Jones, L. R. Whitby, M. M. R. P. Surakattula, H. Huang, H. Shi, J. H. Choi, K. W. Wang, et al. 2016. TLR4/MD-2 activation by a synthetic agonist with no similarity to LPS. *Proc. Natl. Acad. Sci. USA* 113: E884–E893.
- Gao, M., N. London, K. Cheng, R. Tamura, J. Jin, O. Schueler-Furman, and H. Yin. 2014. Rationally designed macrocyclic peptides as synergistic agonists of LPS-induced inflammatory response. *Tetrahedron* 70: 7664–7668.
- Shanmugam, A., S. Rajoria, A. L. George, A. Mittelman, R. Suriano, and R. K. Tiwari. 2012. Synthetic toll like receptor-4 (TLR-4) agonist peptides as a novel class of adjuvants. *PLoS One* 7: e30839.
- Froese, D. S., A. Michaeli, T. J. McCorvie, T. Krojer, M. Sasi, E. Melaev, A. Goldblum, M. Zatsepin, A. Lossos, R. Álvarez, et al. 2015. Structural basis of glycogen branching enzyme deficiency and pharmacologic rescue by rational peptide design. *Hum. Mol. Genet.* 24: 5667–5676.
- Burger-Kentischer, A., I. S. Abele, D. Finkelmeier, K. H. Wiesmüller, and S. Rupp. 2010. A new cell-based innate immune receptor assay for the examination of receptor activity, ligand specificity, signalling pathways and the detection of pyrogens. *J. Immunol. Methods* 358: 93–103.
- Kim, H. M., B. S. Park, J. I. Kim, S. E. Kim, J. G. Paik, H. Lee, and J. O. Lee. 2007. Crystal structure of the TLR4-MD-2 complex with bound endotoxin antagonist Eritoran. *Cell* 130: 906–917.
- Park, B. S., D. H. Song, H. M. Kim, B.-S. Choi, H. Lee, and J.-O. Lee. 2009. The structural basis of lipopolysaccharide recognition by the TLR4-MD-2 complex. *Nature* 458: 1191–1195.
- Kelley, S. L., T. Lukk, S. K. Nair, and R. I. Tapping. 2013. The crystal structure of human soluble CD14 reveals a bent solenoid with a hydrophobic amino-terminal pocket. *J. Immunol.* 190: 1304–1311.
- Kim, J. I., C. J. Lee, M. S. Jin, C. H. Lee, S. G. Paik, H. Lee, and J. O. Lee. 2005. Crystal structure of CD14 and its implications for lipopolysaccharide signaling. *J. Biol. Chem.* 280: 11347–11351.
- Jacobson, M. P., D. L. Pincus, C. S. Rapp, T. J. F. Day, B. Honig, D. E. Shaw, and R. A. Friesner. 2004. A hierarchical approach to all-atom protein loop prediction. *Proteins* 55: 351–367.
- Jacobson, Z. Xiang, and B. Honig. 2002. On the role of the crystal environment in determining protein side-chain conformations. *J. Mol. Biol.* 320: 597–608.
- Lerner, I., A. Goldblum, A. Rayan, A. Vardi, and A. Michaeli. 2018. From finance to molecular modeling algorithms: the risk and return heuristic. *Curr. Top. Pept. Protein Res.* 18: 117–131.
- Markowitz, H. 1952. Portfolio selection. *J. Finance* 7: 77–91.
- Zatsepin, M., A. Mattes, S. Rupp, D. Finkelmeier, A. Basu, A. Burger-Kentischer, and A. Goldblum. 2016. Computational discovery and experimental confirmation of TLR9 receptor antagonist leads. *J. Chem. Inf. Model.* 56: 1835–1846.
- Richards, F. J. 1959. A flexible growth function for empirical use. *J. Exp. Bot.* 10: 290–301.
- Jerabek-Willemsen, M., T. Andre, R. Wanner, H. M. Roth, S. Dhur, P. Bassek, and D. Breitsprecher. 2014. MicroScale thermophoresis: interaction analysis and beyond. *J. Mol. Struct.* 1077: 101–113.
- Plach, M. G., K. D. Grasser, and T. Schubert. 2017. MicroScale Thermophoresis as a tool to study protein-peptide interactions in the context of large eukaryotic protein complexes. *Bio Protoc.* 7: e2632.
- Ohto, U., K. Fukase, K. Miyake, and Y. Satow. 2007. Crystal structures of human MD-2 and its complex with antiendotoxin lipid IVa. *Science* 316: 1632–1634.
- Zorzi, A., K. Deyle, and C. Heinis. 2017. Cyclic peptide therapeutics: past, present and future. *Curr. Opin. Chem. Biol.* 38: 24–29.
- Park, B. S., and J.-O. Lee. 2013. Recognition of lipopolysaccharide pattern by TLR4 complexes. *Exp. Mol. Med.* 45: e66.
- Maelfait, J., E. Vercammen, S. Janssens, P. Schotte, M. Haegman, S. Magez, and R. Beyaert. 2008. Stimulation of Toll-like receptor 3 and 4 induces interleukin-1 β maturation by caspase-8. *J. Exp. Med.* 205: 1967–1973.
- Matzinger, P. 1994. Tolerance, danger, and the extended family. *Annu. Rev. Immunol.* 12: 991–1045.
- Seong, S.-Y., and P. Matzinger. 2004. Hydrophobicity: an ancient damage-associated molecular pattern that initiates innate immune responses. *Nat. Rev. Immunol.* 4: 469–478.
- Rifkin, I., E. A. Leadbetter, L. Busconi, G. Viglianti, and A. Marshak-Rothstein. 2005. Toll-like receptors, endogenous ligands, and systemic autoimmune disease. *Immunol. Rev.* 204: 27–42.
- Sloane, J. A., D. Blitz, Z. Margolin, and T. Vartanian. 2010. A clear and present danger: endogenous ligands of Toll-like receptors. *Neuromolecular Med.* 12: 149–163.
- Bianchi, M. E. 2007. DAMPs, PAMPs and alarmins: all we need to know about danger. *J. Leukoc. Biol.* 81: 1–5.
- Mancek-Keber, M. 2014. Inflammation-mediating proteases: structure, function in (patho) physiology and inhibition. *Protein Pept. Lett.* 21: 1209–1229.
- Means, T. K., S. Wang, E. Lien, A. Yoshimura, D. T. Golenbock, and M. J. Fenton. 1999. Human toll-like receptors mediate cellular activation by *Mycobacterium tuberculosis*. *J. Immunol.* 163: 3920–3927.
- Compton, T., E. A. Kurt-Jones, K. W. Boehme, J. Belko, E. Latz, D. T. Golenbock, and R. W. Finberg. 2003. Human cytomegalovirus activates inflammatory cytokine responses via CD14 and Toll-like receptor 2. *J. Virol.* 77: 4588–4596.